Article citation info:
Brukalski M, Wasiewski A, Renski A. Analysis of the influence of adhesion on limit forces transferred between wheels and road. The Archives of Automotive Engineering – Archiwum Motoryzacji. 2018; 80(2): 5-18. http://dx.doi.org/10.14669/AM.VOL80.ART1

ANALYSIS OF THE INFLUENCE OF ADHESION ON LIMIT FORCES TRANSFERRED BETWEEN WHEELS AND ROAD

ANALIZA WPŁYWU PRZYCZEPNOŚCI PRZYLGOWEJ NA GRANICZNE SIŁY NA KOŁACH POJAZDU

MATEUSZ BRUKALSKI[1], ANDRZEJ WĄSIEWSKI[2], ANDRZEJ REŃSKI[3]
Warsaw University of Technology

Summary

Active safety is one of the most important factors determining the development of modern automobiles. Current vehicles are getting more and more safe, at the same time ensuring better performance. Road conditions during ride are varied and changing, just as the distribution of mass on vehicle axles depending on load distribution may change. A typical passenger car has four wheels, by means of which longitudinal and lateral forces are transferred to the road. In this article, the influence of the kind of surface and weather conditions on limit forces on vehicle wheels is shown. For this purpose, Dynamic Square Method was used (DSM). It allows to establish maximum longitudinal forces on vehicle wheels for a given lateral acceleration. DSM ensures acquiring characteristics in the form of isolines with constant values of lateral acceleration obtained for specific values of longitudinal forces on road wheels. Characteristics are within a field limited by a square, hence the

[1] Warsaw University of Technology, Faculty of Automotive and Construction Machinery Engineering, Institute of Vehicles, Section of Automobiles, ul. Narbutta 84, 02-524 Warsaw; e-mail: mateusz.brukalski@simr.pw.edu.pl

[2] Warsaw University of Technology, Faculty of Automotive and Construction Machinery Engineering, Institute of Vehicles, Section of Automobiles, ul. Narbutta 84, 02-524 Warsaw; e-mail: andrzej.wasiewski@simr.pw.edu.pl

[3] Warsaw University of Technology, Faculty of Automotive and Construction Machinery Engineering, Institute of Vehicles, Section of Automobiles, ul. Narbutta 84, 02-524 Warsaw; e-mail: andrzej.renski@simr.pw.edu.pl

name of the method. Analyzing the obtained characteristics, one can determine how changing the value of adhesion coefficient influences values of longitudinal forces on vehicle wheels.

Keywords: vehicle dynamics, longitudinal and lateral forces, adhesion forces, longitudinal and lateral acceleration, distribution of driving force, Dynamic Square Method

Streszczenie

Bezpieczeństwo czynne jest jednym z najważniejszych czynników decydujących o rozwoju współczesnych samochodów. Obecne pojazdy są coraz bezpieczniejsze, ale także zapewniają coraz lepsze osiągi. Warunki drogowe występujące podczas jazdy są często różne i zmienne, podobnie jak zmieniać się może rozkład masy na osie pojazdu w zależności od rozłożenia ładunku. Typowy samochód osobowy ma cztery koła, za pomocą których przenoszone są na drogę siły wzdłużne i poprzeczne. W niniejszym artykule pokazano wpływ rodzaju nawierzchni i warunków atmosferycznych na graniczne siły na kołach pojazdu. Do tego celu wykorzystano metodę Dynamic Square Method (DSM). Pozwala ona na wyznaczenie maksymalnych sił wzdłużnych na kołach pojazdu dla danego przyspieszenia poprzecznego. Metoda DSM zapewnia uzyskanie charakterystyk w postaci izolinii o stałych wartościach przyspieszeń poprzecznych uzyskiwanych dla konkretnych wartości sił wzdłużnych na kołach jezdnych. Charakterystyki mieszczą się w polu ograniczonym czworokątem, od którego prawdopodobnie wywodzi się nazwa metody. Analizując uzyskane charakterystyki można określić, jaki wpływ na wartości sił wzdłużnych na kołach pojazdu ma zmiana wartości współczynnika przyczepności przylgowej.

Słowa kluczowe: dynamika pojazdu, siły wzdłużne i poprzeczne, siły przyczepności, przyspieszenie wzdłużne i poprzeczne, rozdział siły napędowej, Dynamic Square Method

1. Introduction

One of the key factors influencing active safety of vehicle movement is wheel adhesion to the road, and thus the possibility to transfer tangential forces by means of the wheels. Wheel adhesion to the road derives, on the one hand, from the kind of surface and its condition, on the other hand, from properties of tires, characterized by adhesion coefficient. Modern vehicles are equipped with a number of systems regulating these forces. The first of these systems was, introduced in the 1980's, Anti-Lock Braking System (ABS), and then Anti Slip Regulation (ASR) or Traction Control System (TCS). In the mid 90's of the previous century, vehicle designers developed an even more sophisticated system – Electronic Stability Program (ESP). These systems, in which regulation of wheel skidding takes place thanks to the proper control of the braking system, significantly improved the driving safety and the vehicle travel comfort, especially on the roads with low adhesion coefficient.

In the mid 90's of the previous century, the next step was to introduce TV – torque vectoring, which varies the torque to each wheel. It has significant influence, on the one hand, on the improvement of safety, and on the other hand, on better performance. In control of the driving force distribution, Dynamic Square Method is used.

A passenger car has four wheels. Longitudinal and lateral forces, affecting a vehicle in a given moment are significant. Thus, an important aspect is to establish maximum values of these forces and to verify whether adhesion forces are enough to take over these forces, or not.

DSM enables establishing maximum longitudinal forces, possible to be transferred by particular wheels (axles) of a vehicle, with assumed values of lateral acceleration [1, 3]. The dependence among longitudinal forces affecting particular axles is shown by means of level graphs. Based on these characteristics, it is possible to determine what maximum longitudinal forces, and for what lateral acceleration, a given axle may transfer.

Dynamic Square Method was described in detail in article [1], and [2] shows the application of this method to analyze the influence of vehicle parameters on limit forces on road wheels. However, this article will present how limit forces on wheels are influenced by the kind of surface and weather conditions (more specifically – adhesion coefficient), in which the vehicle rides. The analysis was performed for a few kinds of surface, characterized by different values of adhesion coefficients.

2. Dynamic Square Method

Dynamic Square Method (DSM) was first mentioned in 1995. It was used by Mitsubishi engineers – M. Kato, K. Isoda and H. Yuasa [3]. It was later used to devise a system of driving force distribution to vehicle wheels [6, 7 and 8], which in 1996 was applied in a vehicle model of this company. DSM is also used in publications of M. Klomp [4, 5]. As mentioned earlier, the algorithm of DSM operation was described in [1].

In this study, the possibilities of Dynamic Square Method algorithm are shown, on the example of a two-wheel vehicle model [1]. The focus was on studying the influence of adhesion coefficient on limit forces on vehicle wheels. The analyses for the surface with identical adhesion coefficient of front wheel axle μ_{mf} and rear wheel axle μ_{mr} ($\mu_{mf} = \mu_{mr}$) were conducted, as well as for cases where the coefficient is different for the front axle and the rear axle. The latter case may render e.g. a ride on a slippery surface (oil spill, icing, etc.).

The characteristics of limit forces on wheels was performed for a model vehicle, equipped with a four-wheel drive, with parameters shown in Table 2.1 and for the case where the adhesion coefficient for the front axle μ_{mf} and the rear axle μ_{mf} is different ($\mu_{mf} \neq \mu_{mr}$).

Table. 2.1. Specifications of the model vehicle

Vehicle mass m [kg]	1450
Mass on the front axle m_1 [kg]	870
Mass on the rear axle m_2 [kg]	580
Wheelbase l_{12} [m]	2.65
Distance of the front axle from the center of mass l_1 [m]	1.06
Distance of the rear axle from the center of mass l_2 [m]	1.59
Height of the center of mass h [m]	0.53

Table 2.2 shows the ranges of longitudinal forces on wheels of the front (rear) axle $F_{x1(2)}$. Positive values of these longitudinal forces $F_{x1(2)}$ show driving forces $F_{n1(2)}$, whereas negative values of longitudinal forces $F_{x1(2)}$ relate to braking forces $F_{h1(2)}$. The values were chosen like this, in order to use the assumed adhesion.

Table. 2.2. The assumed ranges of driving forces and braking forces for the model vehicle

Driving force on the front wheels F_{n1} [N]	(0; 12 000)
Braking force on the front wheels F_{h1} [N]	(–12 000; 0)
Driving force on the rear wheels F_{n2} [N]	(0; 12 000)
Braking force on the rear wheels F_{h2} [N]	(–7000; 0)

The starting point for calculations using DSM is initial assumption of values of longitudinal forces on vehicle wheels. Based on this, longitudinal acceleration is established, as well as changes in vertical pressures affecting wheels of the front axle and the rear axle. Thanks to this, it is possible to establish adhesion force of each of the axles. If the force is great enough, it will be possible to transfer also the lateral force, which will enable the curvilinear motion of the vehicle. However, if the adhesion force is smaller than the assumed longitudinal force, the longitudinal force with such a value will not be achieved. Based on the established lateral force, the lateral acceleration for the front axle and the rear axle is calculated. The smaller value is chosen. Each pair of forces (which may be realized), corresponding to the given lateral acceleration, constitutes one point on the characteristics. Graphs made by means of Dynamic Square Method consist of thousands of points, which correspond to maximum total values obtained with a given maximum lateral acceleration. The points corresponding to identical values of lateral acceleration are linked to create level graphs.

The graph of limit forces on wheels made according to the specifications of the model vehicle (Tables 2.1 and 2.2), and assuming identical adhesion coefficient of wheels od front and rear axles $\mu_{mf} = \mu_{mr} = 1.0$, was shown in Fig 2.1.

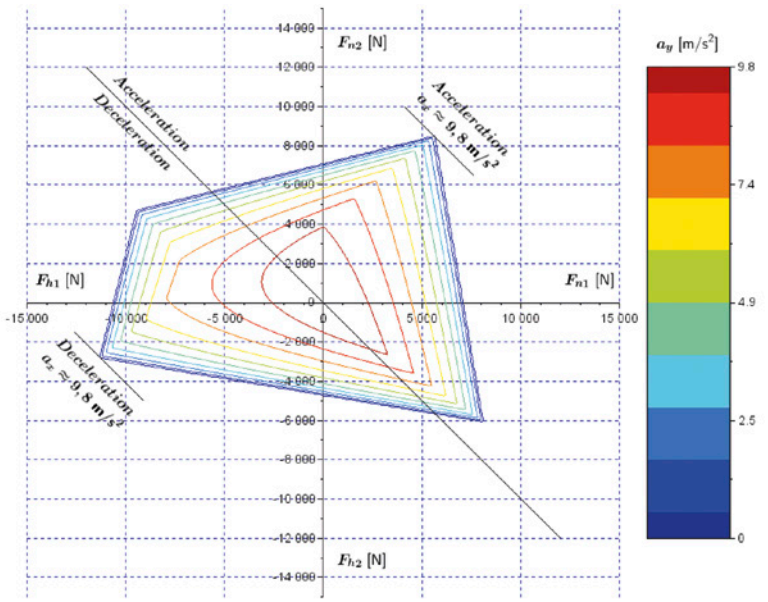

Fig. 2.1. Limit forces on wheels established using DSM for the model vehicle ($h/l_{12} = 0.2$; $\mu_{mf} = \mu_{mr} = 1.0$; $m_1/m_2 = 1.5$) [2]

Characteristics obtained using DSM (Fig. 2.1) allows to establish the maximum values of longitudinal forces on vehicle wheels $F_{x1(2)}$ and the values of lateral acceleration a_y corresponding to them.

Lines angled by 45° towards axis of ordinates correspond to the constants of the total value of longitudinal force on both axles. The maximum total value of driving forces on both axles is then obtained when the lateral acceleration a_y equals zero, and the longitudinal acceleration is maximum ($a_x \approx 9.8$ m/s^2). Values of driving forces for particular axles may be read from the graph (Fig. 2.1), projecting a given point on characteristics envelope onto the axis of ordinates and the axis of abscissae of the characteristics. In an analogical way the maximum total value of braking forces on both axles may be estimated. It is obtained, when lateral acceleration a_y equals zero, and deceleration is maximum ($a_x \approx 9.8$ m/s^2).

For the data assumed in Tables 2.1 and 2.2 for the point of characteristics corresponding to the maximum total value of driving forces on both axles (the upper corner in the positive quarter of the coordinate system), using DSM, the following values of driving forces were obtained: for the front wheels $F_{n1} \approx 5700$ N and for the rear wheels $F_{n2} \approx 8500$ N. For the point of characteristics corresponding to the maximum total value of forces on both axles in case of braking (the bottom corner in the negative quarter of the coordinate system), using DSM, the following values of braking forces were obtained: for the front wheels $F_{h1} \approx -11\,400$ N and for the rear wheels $F_{h2} \approx -2800$ N.

3. The influence of adhesion coefficient and mass distribution on axles

In this point, the influence of adhesion coefficient μ_m on values of limit longitudinal forces on vehicle wheels $F_{x1(2)}$ will be presented. Furthermore, in case of different value of adhesion coefficient of front and rear axle wheels, the influence of mass distribution on axles m_1/m_2 was also considered.

Figures 3.1 and 3.2 show characteristics of limit forces on wheels $F_{x1(2)}$ for two different values of adhesion coefficient obtained using DSM. It was assumed, that the adhesion coefficient of front axle wheels and rear axle wheels is identical and amounts to, respectively $\mu_{mf} = \mu_{mr} = 0.4$ and $\mu_{mf} = \mu_{mr} = 0.6$. Whereas figures 3.3 i 3.4 show characteristics of limit forces on wheels on surface with different adhesion coefficient of front and rear axle wheels ($\mu_{mf} \neq \mu_{mr}$).

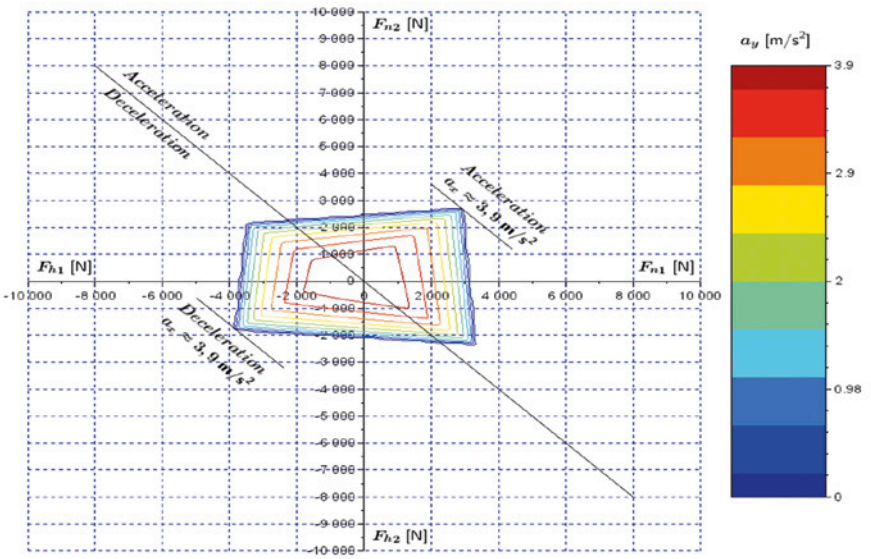

Fig. 3.1. Limit forces on wheels established using DSM for adhesion coefficient $\mu_{mf} = \mu_{mr} = 0.4$ ($h/l_{12} = 0.2$; $m_1/m_2 = 1.5$)

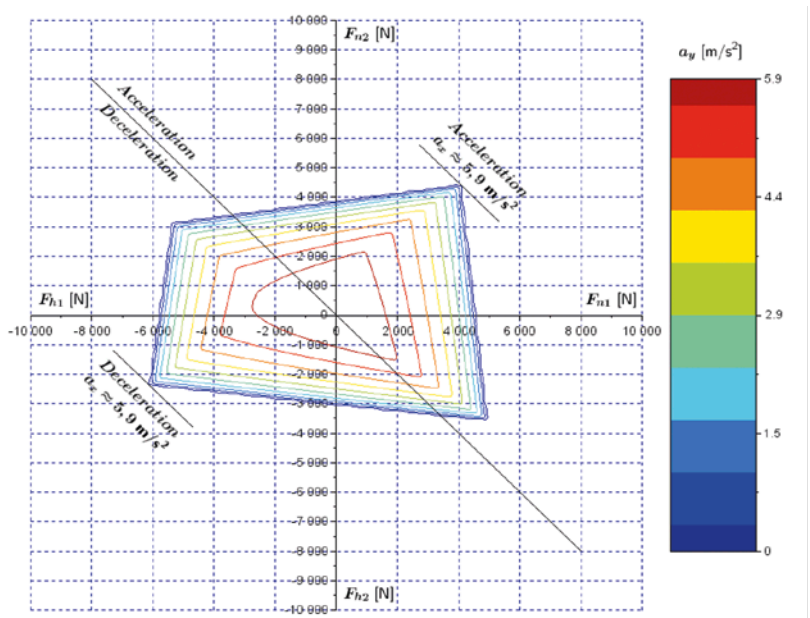

Fig. 3.2. Limit forces on wheels established using DSM for adhesion coefficient $\mu_{mf} = \mu_{mr} = 0.6$ ($h/l_{12} = 0.2$; $m_1/m_2 = 1.5$)

Table 3.1 shows the most important values obtained from characteristics of limit forces on road wheels for the earlier mentioned values of adhesion coefficient.

Table. 3.1. Overview of the most important values obtained from characteristics of limit forces on wheels for different values of an identical adhesion coefficient of front and rear axle wheels and assuming mass distribution $m_1/m_2 = 1.5$

Adhesion coefficient of the wheels	$\mu_{mf} = \mu_{mr} = 1.0$	$\mu_{mf} = \mu_{mr} = 0.6$	$\mu_{mf} = \mu_{mr} = 0.4$
Total driving force on the front wheels[1] F_{n1} [N]	5700 (100%)	4450 (–22%)	2900 (–49%)
Total driving force on the rear wheels[1] F_{n2} [N]	8500 (100%)	4100 (–52%)	2750 (–68%)
Maximum longitudinal acceleration a_x [m/s^2]	9.8 (100%)	5.9 (–40%)	3.9 (–60%)
Total braking force on the front wheels[2] F_{h1} [N]	–11 400 (100%)	–6200 (–46%)	–3850 (–66%)
Total braking force on the rear wheels[2] F_{h2} [N]	–2800 (100%)	–2350 (–16%)	–1800 (–36%)
Maximum deceleration a_x [m/s^2]	9.8 (100%)	5.9 (–40%)	3.9 (–60%)
Maximum lateral acceleration a_y [m/s^2]	9.8 (100%)	5.9 (–40%)	3.9 (–60%)

Decreasing adhesion coefficient of front and rear axle wheels from $\mu_{mf} = \mu_{mr} = 1.0$ to $\mu_{mf} = \mu_{mr} = 0.6$, and then to $\mu_{mf} = \mu_{mr} = 0.4$ results in the decrease of values such as: total driving force on front and rear wheels, maximum longitudinal acceleration, total braking force on front and rear wheel, maximum deceleration, maximum lateral acceleration. It is worth mentioning that decreasing forces is not proportional to decreasing adhesion coefficient. Values expressed in percentage shown in Figure 3.1 indicate increase (+) or decrease (-) of these values in relation to corresponding values for the model vehicle riding on the surface with homogenous adhesion coefficient of front and rear axle wheels $\mu_{mf} = \mu_{mr} = 1.0$ (assumed as 100%).

Figures 3.3 and 3.4 show the influence of surface with different adhesion coefficient of front and rear axle wheels on obtained limit forces on vehicle wheels. Figure 3.3 shows values of limit forces on vehicle road wheels in the situation where adhesion coefficient of rear axle wheels is greater than adhesion coefficient of front axle wheels ($\mu_{mf} = 0.4$ and $\mu_{mr} = 1.0$). Whereas Figure 3.4 shows values of limit forces on vehicle wheels in the situation where, adhesion coefficient of front wheels is greater than adhesion coefficient of rear wheels ($\mu_{mf} = 1.0$ and $\mu_{mr} = 0.4$).

[1] Driving forces in the point of characteristics, in which maximum possible longitudinal acceleration is achieved.

[2] Braking forces in the point of characteristics, in which maximum possible deceleration is achieved.

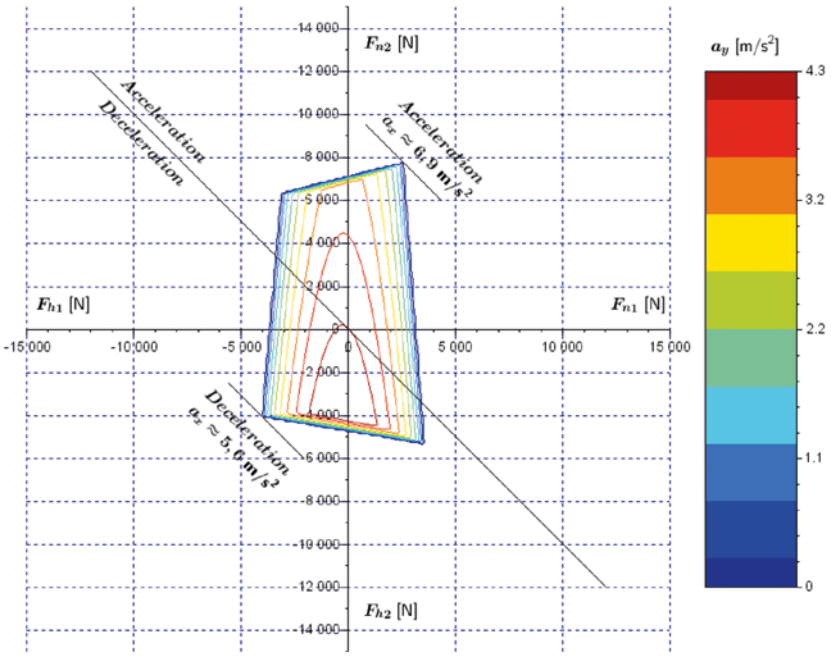

Fig. 3.3. Limit forces on wheels established using DSM for different values of adhesion coefficient on the front axle $\mu_{mf} = 0.4$ and the rear axle $\mu_{mr} = 1.0$ ($h/l_{12} = 0.2$; $m_1/m_2 = 1.5$)

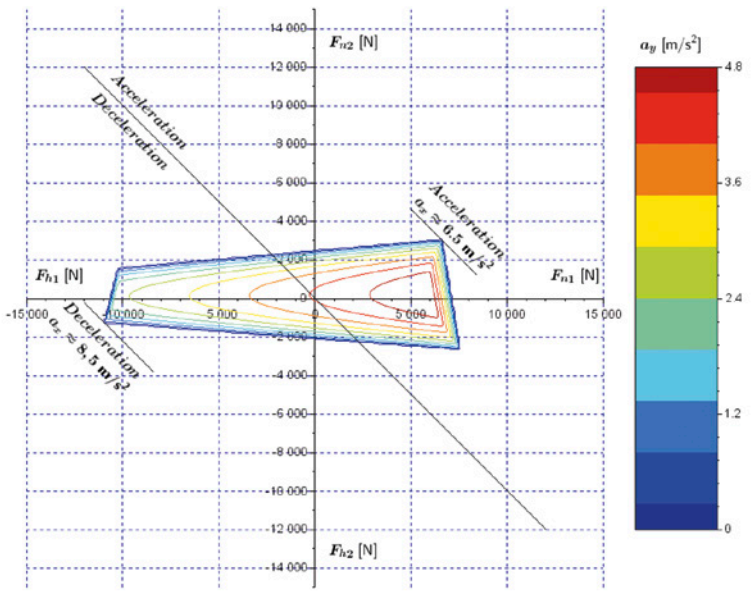

Fig. 3.4. Limit forces on wheels established using DSM for different values of adhesion coefficient on the front axle $\mu_{mf} = 1.0$ and the rear axle $\mu_{mr} = 0.4$ ($h/l_{12} = 0.2$; $m_1/m_2 = 1.5$)

It was also studied how limit coefficient forces $F_{\mu 1(2)}$ on front and rear axle wheels change, in case of surface with different adhesion coefficient of wheels of a given axle $\mu_{mf(r)}$, if the distribution of mass on axles changes.[3]

Figures 3.5 and 3.6 show the influence of surface with different adhesion coefficient of front and rear axle wheels on limit forces vehicle wheels for distribution of mass on axles $m_1/m_2 = 1.0$. Whereas Figures 3.7 and 3.8 show the influence of surface with different adhesion coefficient of front and rear axle wheels for distribution of mass on axles $m_1/m_2 = 0.67$.

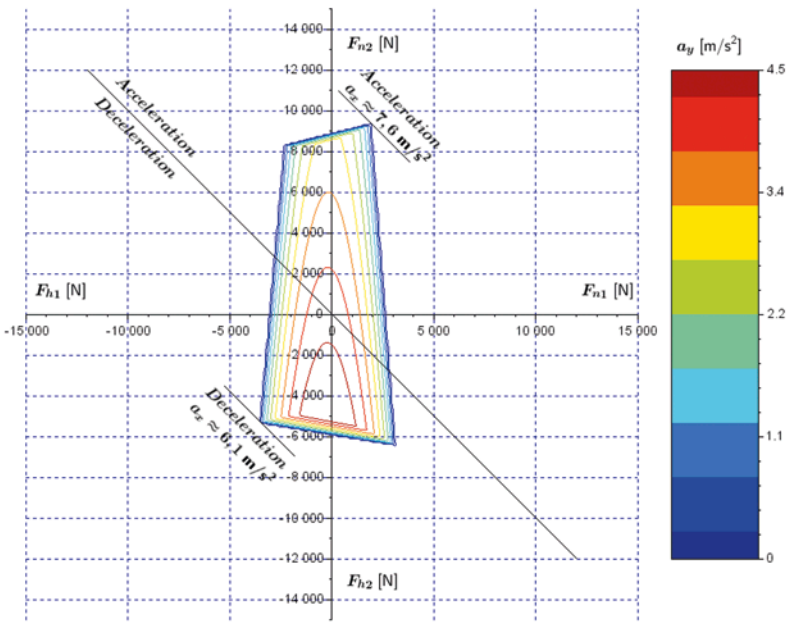

Fig. 3.5. Limit forces on wheels established using DSM for different values of adhesion coefficient on the front axle $\mu_{mf} = 0.4$ and the rear axle $\mu_{mr} = 1.0$ ($h/l_{12} = 0.2$; $m_1/m_2 = 1.0$)

[3] In order to simplify the considerations, it was assumed that the remaining parameters of the vehicle remain the same as those of the model vehicle (Table 2.1).

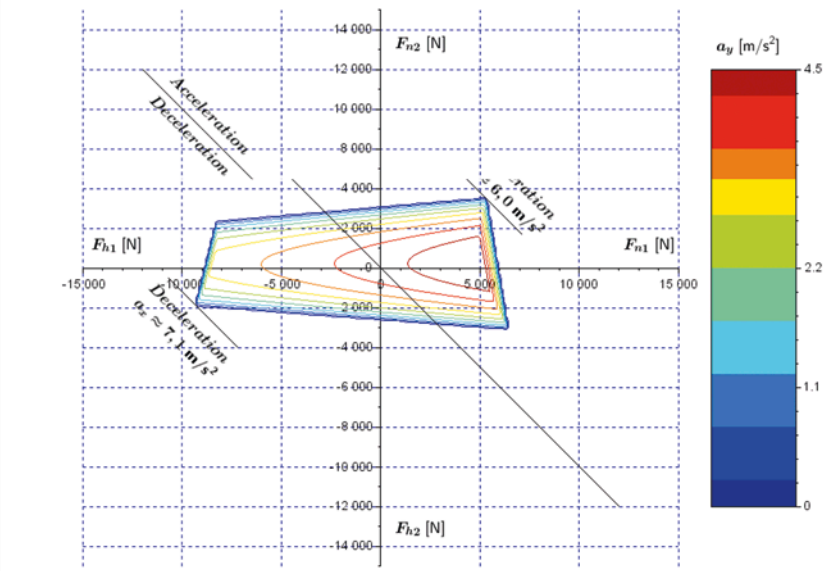

Fig. 3.6. Limit forces on wheels established using DSM for different values of adhesion coefficient on the front axle $\mu_{mf} = 1.0$ and the rear axle $\mu_{mr} = 0.4$ ($h/l_{12} = 0.2$; $m_1/m_2 = 1.0$)

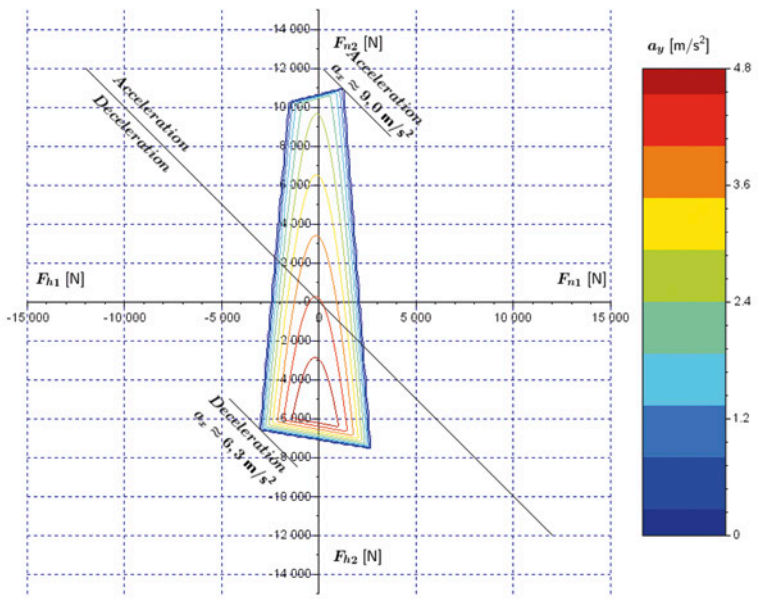

Fig. 3.7. Limit forces on wheels established using DSM for different values of adhesion coefficient on the front axle $\mu_{mf} = 0.4$ and the rear axle $\mu_{mr} = 1.0$ ($h/l_{12} = 0.2$; $m_1/m_2 = 0.67$)

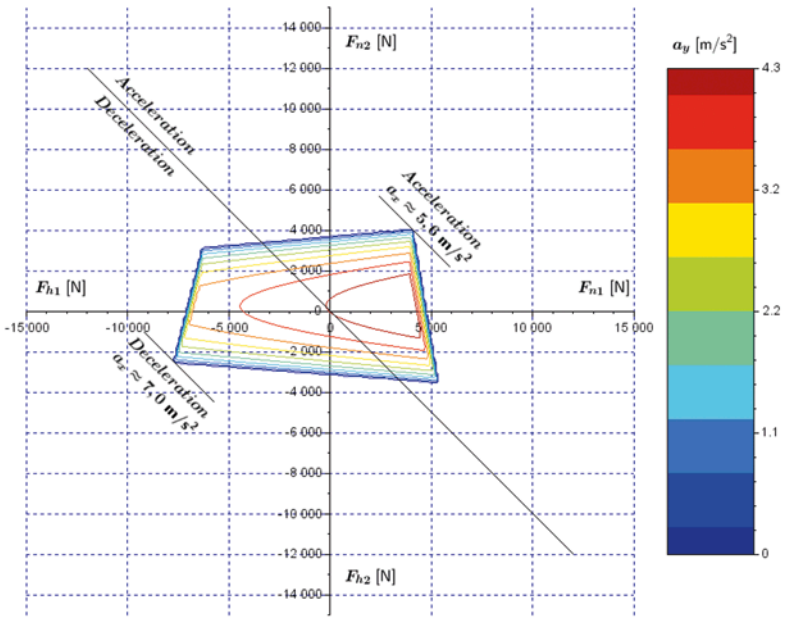

Fig. 3.8. Limit forces on wheels established using DSM for different values of adhesion coefficient on the front axle $\mu_{mf} = 1.0$ and the rear axle $\mu_{mr} = 0.4$ ($h/l_{12} = 0.2$; $m_1/m_2 = 0.67$)

Table. 3.2. Comparison of the most important values obtained from characteristics of limit forces on wheels for different values of adhesion coefficient of the front and rear axles and different distributions of mass on axles ($m_1/m_2 = 1.5$; $m_1/m_2 = 1.0$; $m_1/m_2 = 0.67$)

Adhesion coefficient of the wheels	$\mu_{mf} = 0.4$ $\mu_{mr} = 1.0$ ($m_1/m_2 =$ 1.5)	$\mu_{mf} = 1.0$ $\mu_{mr} = 0.4$ ($m_1/m_2 =$ 1.5)	$\mu_{mf} = 0.4$ $\mu_{mr} = 1.0$ ($m_1/m_2 =$ 1.0)	$\mu_{mf} =1.0$ $\mu_{mr} = 0.4$ ($m_1/m_2 =$ 1.0)	$\mu_{mf} = 0.4$ $\mu_{mr} = 1.0$ ($m_1/m_2 =$ 0.67)	$\mu_{mf} = 1.0$ $\mu_{mr} = 0.4$ ($m_1/m_2 =$ 0.67)
Total driving force on the front wheels[4] F_{n1} [N]	2300 (– 60%)	6400 (+ 12%)	1950 (– 66%)	5200 (– 9%)	2200 (– 61%)	4050 (– 29%)
Total driving force on the rear wheels[4] F_{n2} [N]	7700 (– 9%)	3000 (– 65%)	9450 (+ 11%)	3500 (– 59%)	10 900 (+ 28%)	4000 (– 53%)
Maximum longitudinal acceleration a_x [m/s²]	6.9 (– 30%)	6.5 (– 34%)	7.6 (– 22%)	6.0 (– 39%)	9.0 (– 8%)	5.6 (– 43%)

[4] Driving forces in the point of characteristics, in which maximum possible longitudinal acceleration is achieved.

Table. 3.2. Comparison of the most important values obtained from characteristics of limit forces on wheels for different values of adhesion coefficient of the front and rear axles and different distributions of mass on axles ($m_1/m_2 = 1.5$; $m_1/m_2 = 1.0$; $m_1/m_2 = 0.67$), cont.

Total braking force on the front wheels[5] F_{h1} [N]	– 4050 (– 64%)	– 11 000 (– 4%)	– 3500 (– 69%)	– 9250 (– 19%)	– 2500 (– 78%)	– 7700 (– 32%)
Total braking force on the rear wheels[5] F_{h2} [N]	– 4050 (+ 45%)	– 1300 (– 54%)	– 5350 (+ 91%)	– 1950 (– 30%)	– 6600 (+ 136%)	– 2500 (– 11%)
Maximum deceleration a_x [m/s^2]	5.6 (– 43%)	8.5 (– 13%)	6.1 (– 38%)	7.1 (– 28%)	6.3 (– 36%)	7.0 (– 29%)
Maximum lateral acceleration a_y [m/s^2]	4.3 (– 56%)	4.8 (– 51%)	4.5 (– 54%)	4.5 (– 54%)	4.8 (– 51%)	4.3 (– 56%)

The values expressed in percentage shown in Table 3.2 indicate the increase (+) or the decrease (-) of these values in relation to the corresponding values for the model vehicle riding on the surface with homogenous adhesion coefficient of the front and rear axle wheels $\mu_{mf} = \mu_{mr} = 1.0$ (assumed as 100% – see Table 3.1).

For the mass distribution on axles $m_1/m_2 = 1.5$ for the surface with adhesion coefficient of the front wheels $\mu_{mf} = 0.4$ and adhesion coefficient of the rear wheels $\mu_{mr} = 1.0$ in relation to the model vehicle, the following was noted:

- decrease in total driving force on the front wheels by 60%, and decrease in total driving force on rear wheels by 9%,
- decrease in total braking force on front wheels by 64%, and increase in total braking force on rear wheels by 45%.

For the mass distribution on axles $m_1/m_2 = 1.5$ for the surface with adhesion coefficient of the front wheels $\mu_{mf} = 1.0$ and adhesion coefficient of the rear wheels $\mu_{mr} = 0.4$ in relation to the model vehicle, the following was noted:

- increase in total driving force on the front wheels by 12%, and decrease in total driving force on rear wheels by 65%,
- decrease in total braking force on front wheels by 4%, and decrease in total braking force on rear wheels 54%.

Change in mass distribution on axles from $m_1/m_2 = 1.5$ to $m_1/m_2 = 1.0$ for the surface with adhesion coefficient of the front wheels $\mu_{mf} = 0.4$ and adhesion coefficient of the rear wheels $\mu_{mr} = 1.0$ results in:

- decrease in total driving force on the front wheels by 66%, and increase in total driving force on rear wheels by 11% in relation to the model vehicle,

[5] Braking forces in the point of characteristics, in which maximum possible deceleration is achieved.

- decrease in total braking force on front wheels by 69%, and increase in total braking force on rear wheels by 91% in relation to the model vehicle.

Change in mass distribution on axles from $m_1/m_2 = 1.5$ to $m_1/m_2 = 1.0$ for the surface with adhesion coefficient of the front wheels $\mu_{mf} = 1.0$ and adhesion coefficient of the rear wheels $\mu_{mr} = 0.4$ results in:

- decrease in total driving force on the front wheels by 9%, and decrease in total driving force on rear wheels by 59% in relation to the model vehicle,
- decrease in total braking force on front wheels by 19%, and decrease in total braking force on rear wheels by 30% in relation to the model vehicle.

Change in mass distribution on axles from $m_1/m_2 = 1.5$ to $m_1/m_2 = 0.67$ for the surface with adhesion coefficient of the front wheels $\mu_{mf} = 0.4$ and adhesion coefficient of the rear wheels $\mu_{mr} = 1.0$ results in:

- decrease in total force on the front wheels by 61%, and increase in total driving force on rear wheels by 28% in relation to the model vehicle,
- decrease in total braking force on front wheels by 78%, and increase in total braking force on rear wheels by 136% in relation to the model vehicle.

Change in mass distribution on axles from $m_1/m_2 = 1.5$ to $m_1/m_2 = 0.67$ for the surface with adhesion coefficient of the front wheels $\mu_{mf} = 1.0$ and adhesion coefficient of the rear wheels $\mu_{mr} = 0.4$ results in:

- decrease in total driving force on the front wheels by 29%, and decrease in total driving force on rear wheels by 53% in relation to the model vehicle,
- decrease in total braking force on front wheels by 32%, and decrease in total braking force on rear wheels by 11% in relation to the model vehicle.

4. Summary

In this article, the influence of adhesion coefficient on limit forces on vehicle wheels was presented, using Dynamic Square Method (DSM). Characteristics of limit longitudinal forces on wheels for given values of lateral acceleration, for three different values of adhesion coefficient of the front and rear axle wheels ($\mu_{mf} = \mu_{mr} = 1.0$; $\mu_{mf} = \mu_{mr} = 0.4$; $\mu_{mf} = \mu_{mr} = 0.6$), were performed. The identical adhesion of wheels of both axles was assumed. Furthermore, the influence of the surface with different adhesion coefficient of the front and rear axle wheels on obtained limit forces on vehicle wheels, with constant mass distribution on axles, was shown. In the study, the adhesion coefficient of the front wheels was being decreased to the value of $\mu_{mf} = 0.4$, while keeping the adhesion coefficient of the rear wheels at $\mu_{mr} = 1.0$, and next the adhesion coefficient of the rear wheels was being decreased to the value of $\mu_{mr} = 0.4$, while keeping the adhesion coefficient of the front wheels at $\mu_{mf} = 1.0$. The obtained results were related to the model vehicle riding on a homogenous surface with identical adhesion coefficient of front and rear axle wheels $\mu_{mf} = \mu_{mr} = 1.0$. The influence of vehicle mass distribution on limit forces on wheels, for the case where adhesion coefficient of front and rear axle wheels is different, was also presented.

The conducted analysis confirms the significant influence of adhesion coefficient of wheels and distribution of mass on axles on values of limit longitudinal forces on wheels, and applying DSM allows to establish quantitative dependencies. The results of calculations (analyses) performed in this manner may prove useful while designing active safety systems.

The full text of the article is available in Polish online on the website http://archiwummotoryzacji.pl.

Tekst artykułu w polskiej wersji językowej dostępny jest na stronie http://archiwummotoryzacji.pl.

5. References

[1] Brukalski M. Introduction to dynamic square method. Zeszyty Naukowe Instytutu Pojazdów. 2015; 3(103): 29-35.

[2] Brukalski M. The analysis of the impact of selected vehicle parameters on the limit forces on the vehicle's drive wheels. The Archives of Automotive Engineering – Archiwum Motoryzacji. 2017; 2(76): 5-16.

[3] Kato M, Isoda K, Yuasa H: Study on vehicle dynamics in marginal condition using dynamic square method. SAE Technical Paper. 1995; no 9531020: 69-74.

[4] Klomp M. Passenger Car All-Wheel Drive Systems Analysis. Degree Project University of Trollhättan/Uddevalla. Sweden: 2004.

[5] Klomp M. On Drive Force Distribution and Road Vehicle Handling-A Study of Understeer and Lateral Grip. Chalmers University of Technology. Sweden: 2007.

[6] Sawase K, Ushiroda Y, Inoue K. Effect of the Right-and-left Torque Vectoring System in Various Types of Drivetrain. SAE Technical Paper. 2007; 2007-01-3645: 1-8. doi:10.4271/2007-01-3645.

[7] Sawase K, Ushiroda Y. Improvement of Vehicle Dynamics by Right-and-Left Torque Vectoring System in Various Drivetrains. Mitsubishi Motors Technical Review. 2008; no 20: 14-20.

[8] Ushiroda Y, Sawase K, Takahashi N, Suzuki K, Manabe K. Development of Super AYC. Technical Review. 2003; no 15: 73-76.

Article citation info:
Chlopek Z, Strzalkowska K. Research on the impact of automotive sources on the immission of specific size fractions of particulate matter in a street canyon. The Archives of Automotive Engineering – Archiwum Motoryzacji. 2018; 80(2): 19-35. http://dx.doi.org/10.14669/AM.VOL80.ART2

RESEARCH ON THE IMPACT OF AUTOMOTIVE SOURCES ON THE IMMISSION OF SPECIFIC SIZE FRACTIONS OF PARTICULATE MATTER IN A STREET CANYON

BADANIA WPŁYWU ŹRÓDEŁ MOTORYZACYJNYCH NA IMISJĘ FRAKCJI WYMIAROWYCH CZĄSTEK STAŁYCH W KANIONIE ULICZNYM

ZDZISŁAW CHŁOPEK[1], KATARZYNA STRZAŁKOWSKA[2]

Warsaw University of Technology
Automotive Industry Institute (PIMOT)

Summary

The article presents results of empirical survey of the immission of specific size fractions of particulate matter as well as carbon monoxide and nitrogen oxides in the street canyon area in Warsaw in a summer month. The data characterizing the weather conditions and motor vehicle traffic intensity, collected during the survey, were also examined. The data subjected to the analysis included measurement results obtained from the "Warszawa-Komunikacyjna" Air Quality Monitoring Station in Warsaw at Aleja Niepodległości 227/233 and results of measurements carried out at the same place

[1] Warsaw University of Technology, Faculty of Automotive and Construction Machinery Engineering, Institute of Vehicles, ul. Narbutta 84, 02-524 Warszawa, Poland; e-mail: zdzislaw.chlopek@simr.pw.edu.pl

[2] Automotive Industry Institute (PIMOT), Material Testing Laboratory, ul. Jagiellońska 55, 01-301 Warszawa, Poland; e-mail: k.strzalkowska@pimot.eu

by PIMOT with the use of a TSI dust meter. The immission of the PM10, PM2.5, and PM1 particulate matter fractions was examined. It was found that automotive sources exerted a marked impact on the immission of various particulate matter size fractions, especially fine dusts. The correlational interdependence between the immission of particulate matter PM10 and the immission of nitrogen dioxide and carbon monoxide was also studied, based on results of measurements carried out at the Air Quality Monitoring Station. The correlation was found to be weak, probably because of the measurement method used. The correlational examination of the immission of individual particulate matter size fractions, based on measurement results obtained with using a dust meter, showed the correlation to be very strong. In general, pollutant emission from motor vehicles was found to have a considerable impact on the particulate matter immission in the street canyon area, especially on the immission of fine dust fractions.

Keywords: pollutant immission, particulate matter, motorization, street canyon

Streszczenie

W artykule przedstawiono wyniki badań empirycznych imisji frakcji wymiarowych pyłów oraz tlenku węgla i tlenków azotu w okolicach kanionu ulicznego w Warszawie w miesiącu letnim. Badano również wyniki charakteryzujące warunki atmosferyczne oraz natężenie ruchu samochodów. Do analizy wykorzystano wyniki badań, wykonywanych na stacji nadzorowania jakości powietrza Warszawa-Komunikacyjna przy Al. Niepodległości 227/233, oraz przeprowadzanych przy użyciu pyłomierza firmy TSI. Badano imisję frakcji wymiarowych cząstek stałych: PM10, PM2.5 i PM1. Stwierdzono wyraźny wpływ źródeł motoryzacyjnych na imisję frakcji wymiarowych pyłów, szczególnie pyłów drobnych. Badano również zależność korelacyjną imisji zanieczyszczeń cząstek stałych PM10 oraz dwutlenku azotu i tlenku węgla – na podstawie wyników badań na stacji nadzorowania jakości powietrza. Stwierdzono słabą korelację, co wynikało prawdopodobnie z zastosowanej metodyki pomiarów. Badania korelacyjne imisji frakcji wymiarowych cząstek stałych, wykonane na podstawie wyników badań wykonanych przy użyciu pyłomierza, wykazały bardzo silną korelację. Ogólnie stwierdzono istotny wpływ emisji zanieczyszczeń z pojazdów samochodowych na imisję cząstek stałych w kanionie ulicznym, szczególnie na imisje drobnych frakcji wymiarowych pyłów.

Słowa kluczowe: imisja zanieczyszczeń, cząstki stałe, motoryzacja, kanion uliczny

1. Introduction

The pollution of atmospheric air is a very serious problem, especially in large urban agglomerations. The pollutants may be both gaseous and particulate. Dust is defined as the dispersed phase of a two-phase system consisting of a solid body, i.e. small solid particles, suspended in gaseous dispersion medium. In general, dust is a mixture of particulate matter suspended in atmospheric air [5–9, 11, 15, 16].

The particulate matter may be categorized in respect of the equivalent particle size, which depends on the aerodynamic equivalent diameter (AED) of the particle. The following particulate matter fractions are usually discerned [1–5, 7, 8, 10, 11, 15–17]:

- TSP (total suspended particles), with AED below 300 μm,
- fine dust PM10, with AED below 10 μm,
- fine dust PM2.5, suspended particulate matter with AED below 2.5 μm,

– dust PM1, with AED below 1 μm, taken in consideration at the testing of internal combustion engines.

Particulate pollutants have a considerable impact on human health. This impact depends on particle size, shape, and chemical composition. The dust most dangerous to human health is the fine-grained particulate matter because it reaches the deepest portions of the human respiratory system, where it accumulates and, in a part, is absorbed. Moreover, the finest dusts penetrate into the cardiovascular system and thus, they may spread all over the organism; in particular, they may reach the brain [5, 7–9, 12, 13, 15, 16].

2. Methods of the research

The research was undertaken to assess the impact of automotive sources of pollutant emission on the values of immission of individual particulate matter size fractions in the atmospheric air in the street canyon in the Warsaw urban agglomeration.

The models of immission (I) of particulate matter PM2.5 and PM1 are built in accordance with the functional similarity criterion [1–3, 7, 8], with using the definitions of individual dust categories. The set of dusts with AED below 2.5 μm, i.e. PM2.5, is treated as a subset of the set of particulate matter with AED below 10 μm (PM10) and the particulate matter PM1 constitutes a subset of the set defined as PM2.5. The immission of particulate matter PM2.5 is modelled as linearly dependent on the immission of the PM10 dust [1–3, 5, 10, 14]:

$$I_{PM2.5} = k_{PM2.5-PM10} \cdot I_{PM10} \tag{1}$$

where $k_{PM2.5\text{-}PM10}$ – coefficient of the model of immission of the PM2.5 dust ($k_{PM2.5\text{-}PM10} \in \langle 0;1 \rangle$).

The immission of particulate matter PM1 is modelled as linearly dependent on the PM2.5 immission [1, 3, 10, 14]:

$$I_{PM1} = k_{PM1-PM2.5} \cdot I_{PM2.5} \tag{2}$$

where $k_{PM1\text{-}PM2.5}$ – coefficient of the model of immission of the PM1 dust ($k_{PM1\text{-}PM2.5} \in \langle 0;1 \rangle$).

The PM1 dust is also a subset of the PM10 particulate matter; therefore, its immission may also be modelled as linearly dependent on the immission of the PM10 dust [1, 3, 10, 14]:

$$I_{PM1} = k_{PM1-PM10} \cdot I_{PM10} \tag{3}$$

where $k_{PM1\text{-}PM10}$ – coefficient of the model of immission of the PM1 dust ($k_{PM1\text{-}PM10} \in \langle 0;1 \rangle$).

The models of immission of particulate matter PM2.5 and PM1 are identified by determining the model coefficients based on results of empirical measurements [1, 3, 10, 14].

The models of immission of the PM10 particulate matter are also built in accordance with the functional similarity criterion. They include models of immission of the particulate matter with AED below 10 μm where these immission is treated as linearly dependent on the immission of nitrogen oxides (or nitrogen dioxide in some of the said models) or on the immission of carbon monoxide [3, 10, 14]:

$$I_{PM10} = a_{0NOx} + a_{1NOx} \cdot I_{NO_x} \quad (4)$$

$$I_{PM10} = a_{0CO} + a_{1CO} \cdot I_{CO} \quad (5)$$

The measuring stand was located at the "Warszawa-Komunikacyjna" Air Quality Monitoring Station operating within the State Environmental Monitoring. The Station is owned by the Provincial Inspectorate of Environmental Protection (WIOŚ) and located in Warsaw at Aleja Niepodległości 227/233 (Station code: PL0140A), in an urban area, commercial and residential zone. The Station has been situated immediately at the western carriageway of Aleja Niepodległości (leading towards the Ursynów district) [14]. The immission of the following pollutants and the following meteorological characteristics of the atmospheric air are measured at the said Station:

- nitrogen dioxide,
- carbon monoxide,
- suspended particulate matter PM10,
- suspended particulate matter PM2.5,
- benzene,
- 1,2-xylene,
- methylbenzene,
- 1,3-xylene 1,4-xylene,
- ethylbenzene,
- relative humidity,
- air temperature.

Figure 1 shows the measuring stand and the WIOŚ-owned Air Quality Monitoring Station.

Fig. 1. Photographs of the measuring stand and the Air Quality Monitoring Station of the Provincial Inspectorate of Environmental Protection (WIOŚ) [14]

Within this work, the immission of the following particulate matter size fractions was determined [14], with using a TSI dust meter, model 8533/8534 Dust Trak DRX Aerosol Monitor:

- TSP (total suspended particles), i.e. a mixture of particulate matter with equivalent particle size below 300 μm,
- particulate matter PM10 (airborne dust), i.e. particulate matter with equivalent particle size below 10 μm,
- particulate matter PM2.5 (fine dust), i.e. particulate matter with equivalent particle size below 2.5 μm,
- particulate matter PM1 (dust practically invisible to the naked eye), i.e. particulate matter with equivalent particle size below 1 μm.

The particulate matter immission was measured once per minute; then, the measurement results were averaged for a one-hour period. The scope of the survey also included measurements of motor vehicle traffic intensity, with discerning small vehicles (i.e. passenger cars – PC), large vehicles (which included light commercial vehicles – LCV, heavy duty vehicles – HDV, and buses – B), and motorcycles –Mc. The motor vehicle traffic intensity was determined by observations carried out during the pollutant immission measurements. Moreover, current weather conditions, i.e. ambient temperature, air humidity, wind velocity, and precipitations, were monitored [14].

The place of carrying out the measurements was chosen on purpose because the measurement results obtained from the Air Quality Monitoring Station were also analysed [14].

3. Results of empirical measurements

The measurements were carried out in July 2016. In this article, only selected measurement results have been presented, obtained on 5 July 2016 [14].

Figure 2 shows the immission of total suspended particles (TSP), recorded by the Dust Trak DRX Aerosol Monitor; unprocessed data have been presented. The measurements were carried out for a period of 6 h, from 8:15 a.m. till 2:15 p.m., on Tuesday 5 July 2016 [14].

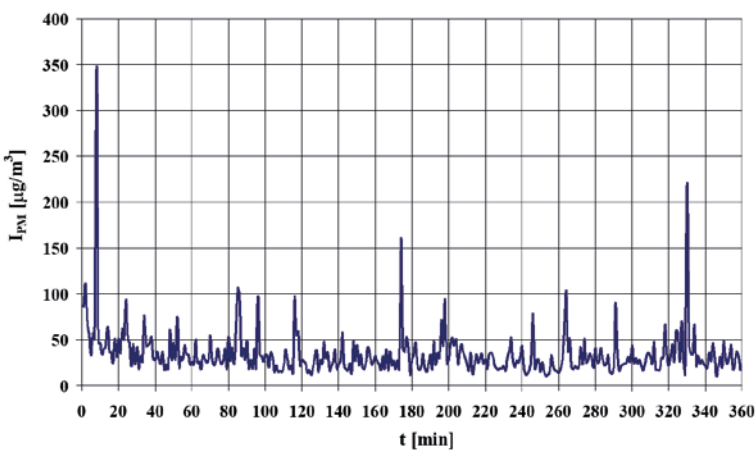

Fig. 2. The TSP immission (unprocessed data recorded by the Dust Trak DRX Aerosol Monitor) [14]

Figure 3 shows the TSP immission, recorded by the Dust Trak DRX Aerosol Monitor; the data were then smoothed by 1st-order and 2nd-order non-recursive filters for the share of high-frequency noise in the signal to be reduced [14]:

$$y(n)=\frac{1}{5}\left[x(n-2)+x(n-1)+x(n)+x(n+1)+x(n+2)\right] \tag{6}$$

$$z(n)=\frac{1}{5}\left[y(n-2)+y(n-1)+y(n)+y(n+1)+y(n+2)\right] \tag{7}$$

where: x – input signal,

y – signal processed by the 1st-order filter,

z – signal processed by the 2nd-order filter (in relation to the input signal),

n – successive number of a signal sample.

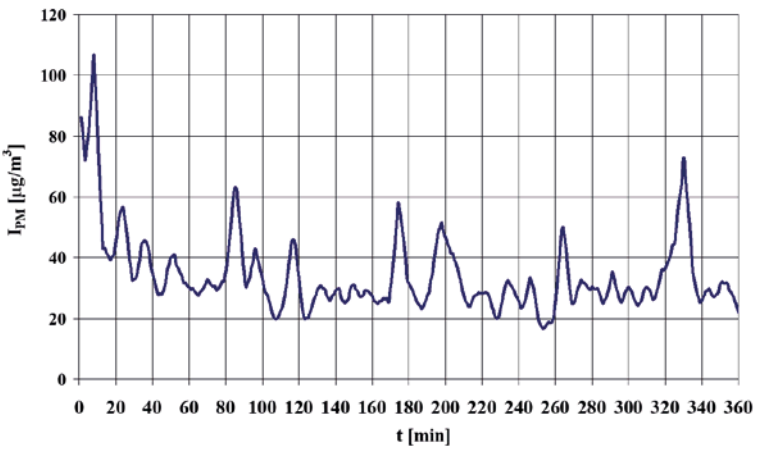

Fig. 3. The TSP immission (data recorded by the Dust Trak DRX Aerosol Monitor and smoothed by filtration) [14]

At the beginning of the measuring period, an increased value of the TSP immission was observed, which might be explained by minor traffic congestions that occurred at that time. The cyclic growths and drops in the TSP immission were caused by changing traffic lights at the intersection of Aleja Niepodległości with ulica Nowowiejska. In the curve shown in figure 3, smoothed with using the 1st-order and 2nd-order non-recursive filters, the cyclic growths and drops in the TSP immission are already not so conspicuous. The marked local peaks, such as the one around the 175th minute of the measuring period, were caused by the passage of a delivery motor vehicle that emitted a considerable amount of exhaust gases [14].

Figure 4 shows the immission of particulate matter PM1, PM2.5, and PM10, recorded by the Dust Trak DRX Aerosol Monitor; unprocessed data have been presented [14].

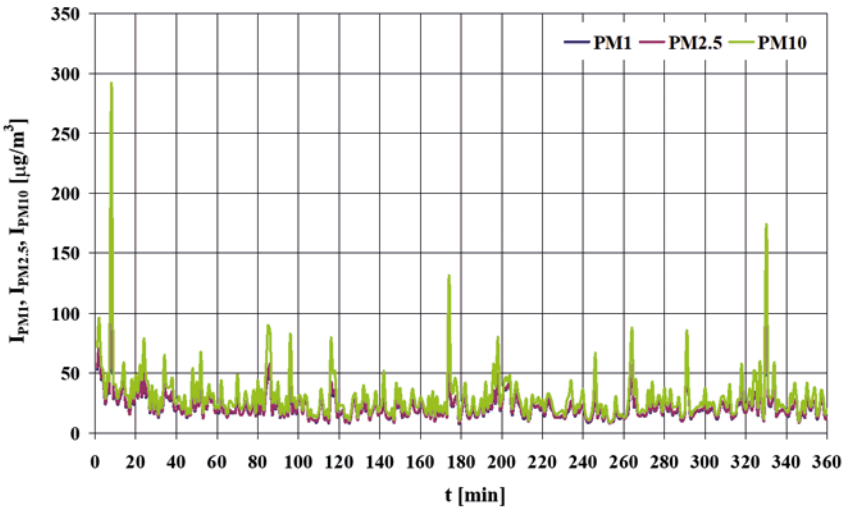

Fig. 4. The immission of particulate matter PM1, PM2.5, and PM10 (unprocessed data recorded by the Dust Trak DRX Aerosol Monitor) [14]

Figure 5 shows the immission of particulate matter PM1, PM2.5, and PM10, recorded by the Dust Trak DRX Aerosol Monitor; then, the data were smoothed by the 1st-order and 2nd-order non-recursive filters for the share of high-frequency noise in the signal to be reduced [14].

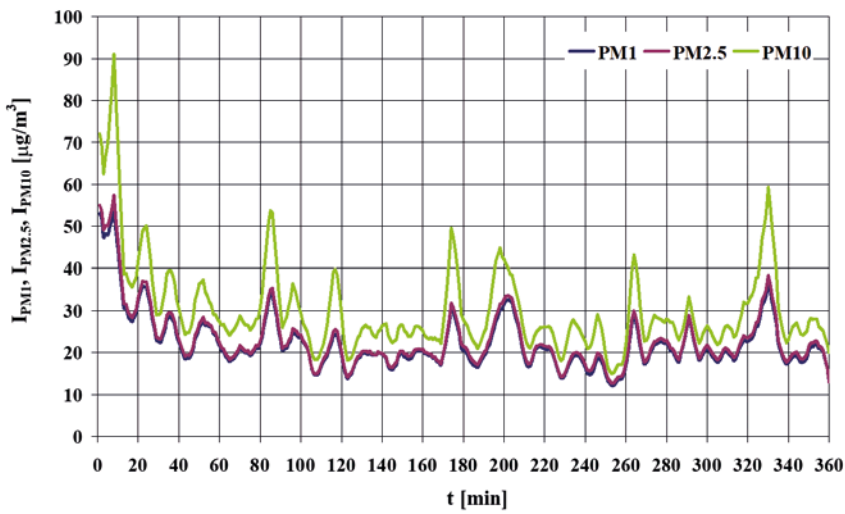

Fig. 5. The immission of particulate matter PM1, PM2.5, and PM10 (data recorded by the Dust Trak DRX Aerosol Monitor and smoothed by filtration) [14]

The immission of particulate matter PM1 and PM2.5 was found to be close to each other. The particulate matter coming from automotive sources chiefly consists of fine-grained material, i.e. the PM1 and PM2.5 dust. The immission of particulate matter PM10 was additionally affected by the secondary stirring up of dust from road surface and reserved track tramway. Such a phenomenon could actually be seen to occur during the measurements [14].

Fig. 6 shows the immission of particulate matter PM2.5 and PM10, obtained from the "Warszawa-Komunikacyjna" WIOŚ-owned Air Quality Monitoring Station and recorded by the Dust Trak DRX Aerosol Monitor; unprocessed data have been presented [14].

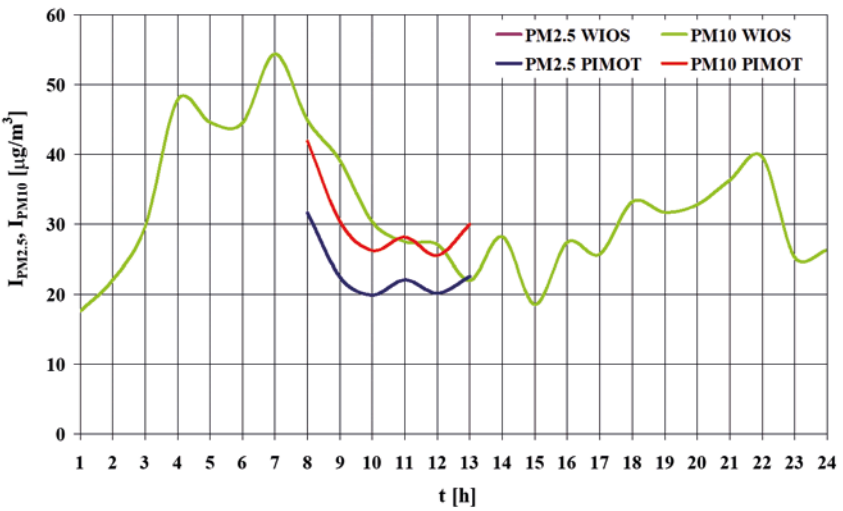

Fig. 6. The immission of particulate matter PM2.5 and PM10 (unprocessed data obtained from the "Warszawa-Komunikacyjna" WIOŚ-owned Air Quality Monitoring Station and recorded by the Dust Trak DRX Aerosol Monitor) [14]

Figure 7 shows the same immission, but the data were smoothed by the 1st-order and 2nd-order non-recursive filters [14].

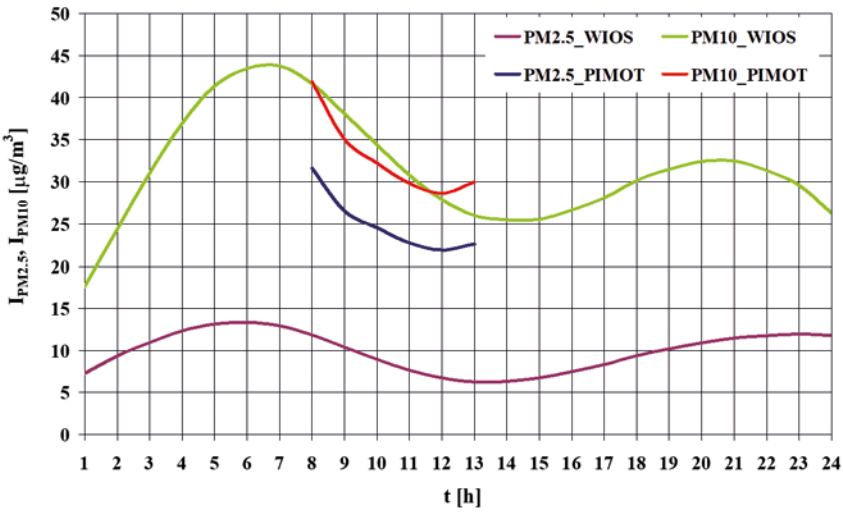

Fig. 7. The immission of particulate matter PM2.5, and PM10 (data obtained from the "Warszawa-Komunikacyjna" WIOŚ-owned Air Quality Monitoring Station and recorded by the Dust Trak DRX Aerosol Monitor; the data were smoothed by filtration) [14]

The results of measurements of the PM10 immission, obtained from the Air Quality Monitoring Station and recorded by the dust meter, do not significantly differ from each other. Conversely, big differences can be seen in the case of particulate matter PM2.5. The reasons for such a finding are difficult for identifying; undoubtedly, however, the very low PM2.5 immission in comparison with the immission of the PM10 dust as reported by the Air Quality Monitoring Station is not typical for the pollutants emitted from automotive sources. For such pollutants, the very fine dust predominates in the whole set of particulate matter [1–3, 5, 7, 8, 10], as it can be seen in the measurement results obtained from the Dust Trak DRX Aerosol Monitor.

Raised PM2.5 and PM10 immission was observed in the morning rush hours; moreover, they were higher again between 8 p.m. and 10 p.m., i.e. after the evening rush hours.

The scope of the survey also included the observation of current weather conditions such as ambient temperature, air humidity, wind velocity, and precipitations. The air temperature and humidity measurement results were obtained from the "Warszawa-Komunikacyjna" WIOŚ-owned Air Quality Monitoring Station. The wind velocity was measured with using a TSI thermal anemometer model 9535 VelociCalc [14].

The results of measurements of temperature (T) and relative humidity (w) of the ambient air have been presented in figure 8.

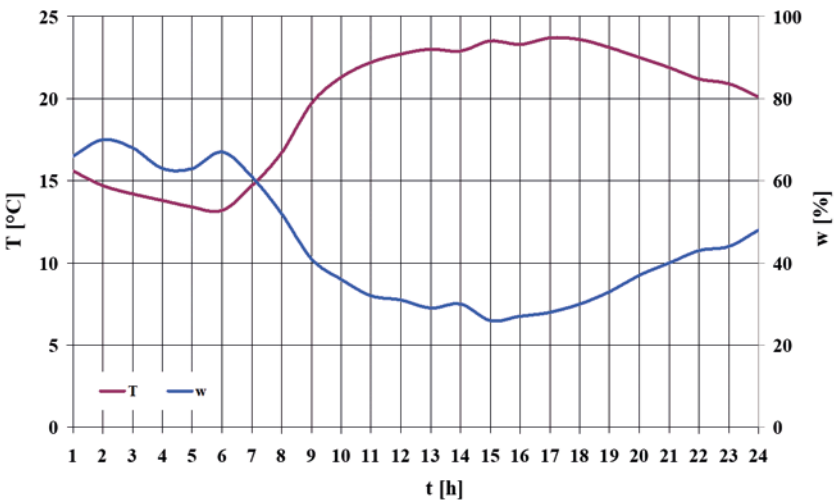

Fig. 8. The temperature (T) and relative humidity (w) of the ambient air (data obtained from the "Warszawa-Komunikacyjna" WIOŚ-owned Air Quality Monitoring Station) [14]

On the day when the measurements were carried out, the ambient temperature was within a range of (13 ÷ 24) °C and the relative humidity varied between 26% and 70%. The average temperature and humidity values did not exceed 20 °C and 45%, respectively. The air temperature and humidity on that day did not have a considerable impact on the particulate matter immission values [14].

The results of measurement of wind velocity and ambient air temperature have been presented in table. Unfortunately, the measurements were not continuously carried out because of limited capabilities of the test equipment available [14].

Table. Wind velocity and ambient air temperature [14]

Time	Wind velocity	Air temperature
h:min:s	m/s	°C
08:16:58	1.67	23.6
08:17:13	1.6	23
08:17:28	0.89	22.8
08:17:55	0.97	22.6
08:18:10	1.12	22.3
09:24:05	1.53	25.8
09:24:20	0.57	24.7
09:24:38	0.82	24.1

Time	Wind velocity	Air temperature
h:min:s	m/s	°C
11:05:32	0.95	28.7
11:05:58	0.17	28.7
11:21:00	0.59	32
11:21:25	0.66	30.7
11:21:48	1.59	27.7
11:22:29	0.55	25.7
12:04:05	1.08	27.5
12:04:26	0.66	26.7

09:24:54	0.65	24
11:04:16	0.49	28.4
11:04:31	1.69	28.6
11:04:47	1.33	28.7
11:05:02	1.31	28.7
11:05:16	0.76	28.7

13:16:16	0.63	26.5
13:16:50	0.32	26.3
13:17:07	0.78	26.2
14:04:13	1.33	25.9
14:04:31	0.74	25.4
08:19:52	0.52	23.1

The average wind velocity was about 0.68 m/s and the wind velocity range was 1.52 m/s. The average air temperature was 27.7 °C and the air temperature range was 9.7 °C. Based on the previous experience gained in the research on particulate matter immission, an assumption may be made that on that day, neither the wind velocity nor the air temperature had any considerable impact on the particulate matter immission values [14].

The scope of the survey also included measurements of motor vehicle traffic intensity N [V/h] (here: V is the number of vehicles) at the place of the measurements. The vehicles moving along Aleja Niepodległości were divided into three groups: the first one consisted of passenger cars – PC, the second one included light commercial vehicles – LCV (i.e. light trucks and delivery vehicles), heavy-duty vehicles – HDV, and buses – B, and the third one comprised motorcycles – Mc. The observations were simultaneously carried out at two carriageways: one leading towards the city centre ("Centrum") and the other one leading in the opposite direction, i.e. towards the Ursynów district. The observation results have been presented in figure 9 [14].

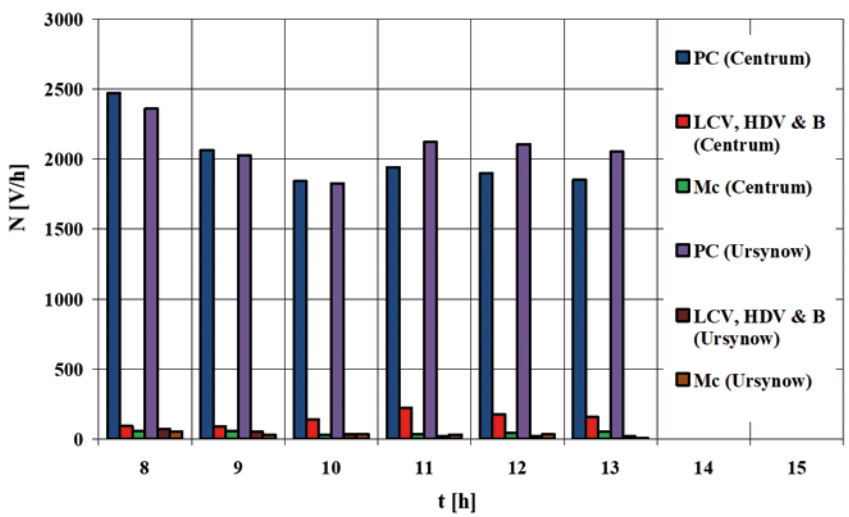

Fig. 9. Intensity of the vehicle traffic in both directions of Aleja Niepodległości [14]

When analysing figure 9, one can notice that both towards the city centre ("Centrum") and towards the Ursynów district, the most vehicles moved in the morning hours, i.e. between

8 a.m. and 9 a.m. The particulate matter immission also reached the highest values during the first hours of carrying out the measurements. This shows that the particulate matter present in the atmosphere in that area was chiefly emitted from motor vehicle traffic [14].

4. Examination of the correlation between the immission of particulate matter PM10 and the immission of nitrogen dioxide and carbon monoxide

The immission of particulate matter PM10 together with the immission of carbon monoxide – CO and nitrogen dioxide – NO_2 have been presented in figure 10. The data were obtained from the "Warszawa-Komunikacyjna" WIOŚ-owned Air Quality Monitoring Station and then the resulting curves were smoothed by the 1st-order and 2nd-order non-recursive filters [14].

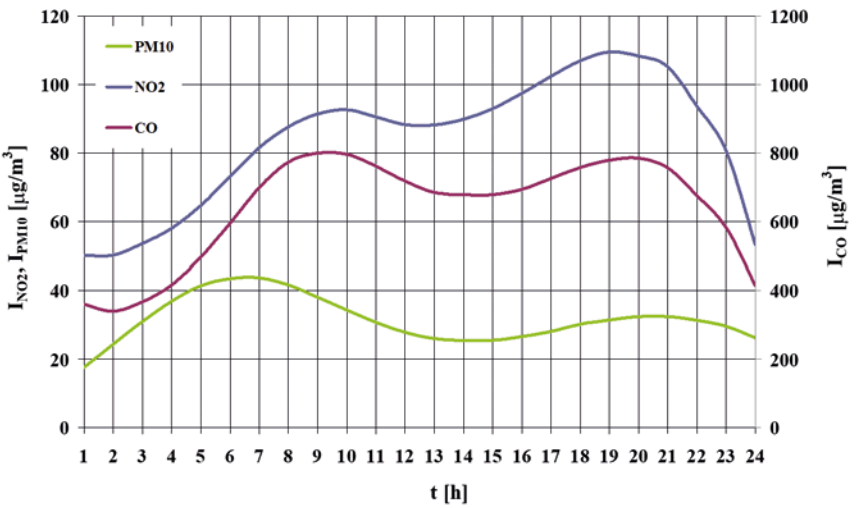

Fig. 10. The immission of particulate matter PM10, carbon monoxide, and nitrogen dioxide (data obtained from the "Warszawa-Komunikacyjna" WIOŚ-owned Air Quality Monitoring Station) [14]

The curves in figure 10 indicate that the immission of carbon monoxide and nitrogen dioxide grew during both the morning and afternoon rush hours [14].

Correlational interdependences between the immission of particulate matter PM10 and carbon monoxide as well as between the immission of particulate matter PM10 and nitrogen dioxide have been presented in figures 11 and 12. The data were obtained from the "Warszawa-Komunikacyjna" WIOŚ-owned Air Quality Monitoring Station [14].

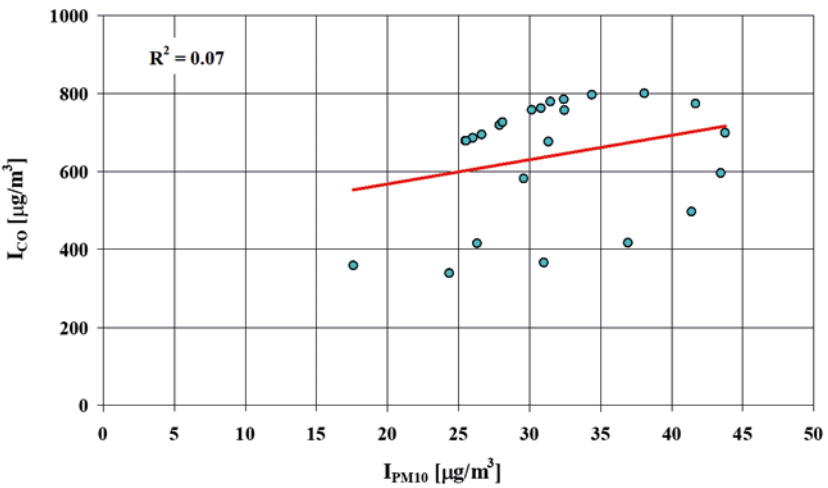

Fig. 11. Correlational interdependence between the immission of particulate matter PM10 and carbon monoxide (data obtained from the "Warszawa-Komunikacyjna" WIOŚ-owned Air Quality Monitoring Station) [14]

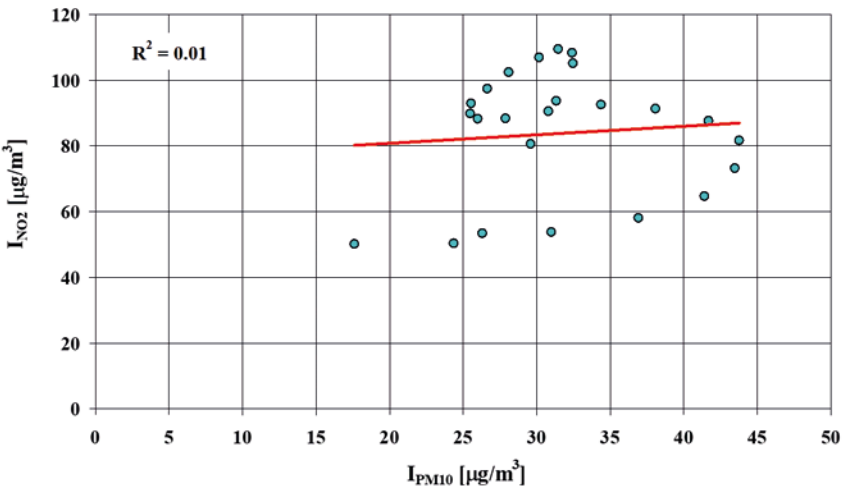

Fig. 12. Correlational interdependence between the immission of particulate matter PM10 and nitrogen dioxide (data obtained from the "Warszawa-Komunikacyjna" WIOŚ-owned Air Quality Monitoring Station) [14]

An analysis of the results presented in figures 11 and 12 did not reveal any considerable correlation between the immission of particulate matter PM10 and carbon monoxide: the value of the coefficient of determination was $R^2 = 0.07$. No correlation was observed, either, between the immission of particulate matter PM10 and nitrogen dioxide: in this case, the value of the coefficient of determination was $R^2 = 0.01$ [14].

These results of the correlational examination of the immission of particulate matter PM10 and the immission of nitrogen dioxide and carbon monoxide, showing the correlation to be weak, may be explained by random errors caused by significant dispersion of the pollutants in the samples taken for measurements as well as by insufficient observation time.

5. Coefficients of the model of immission of specific size fractions of particulate matter

Figures 13 and 14 show processes and mean values of individual coefficients of the model of immission of specific size fractions of particulate matter [14].

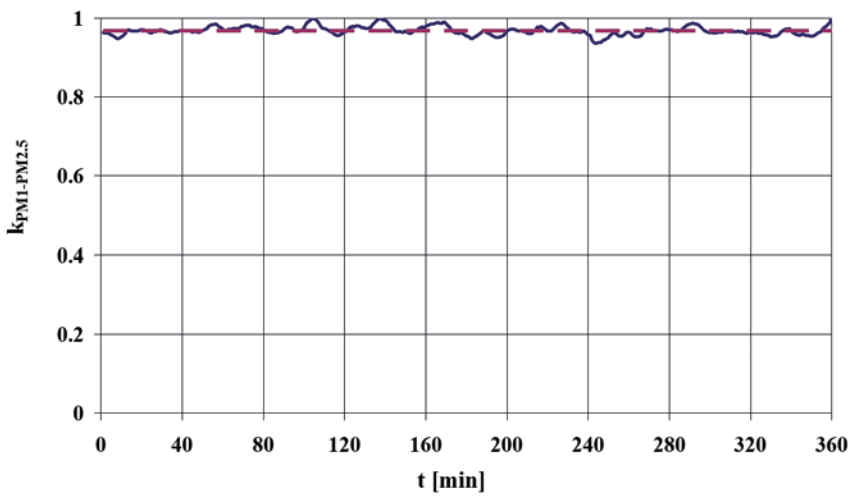

Fig. 13. Coefficient $k_{PM1-PM2.5}$ (data obtained from the Dust Trak DRX Aerosol Monitor) [14]

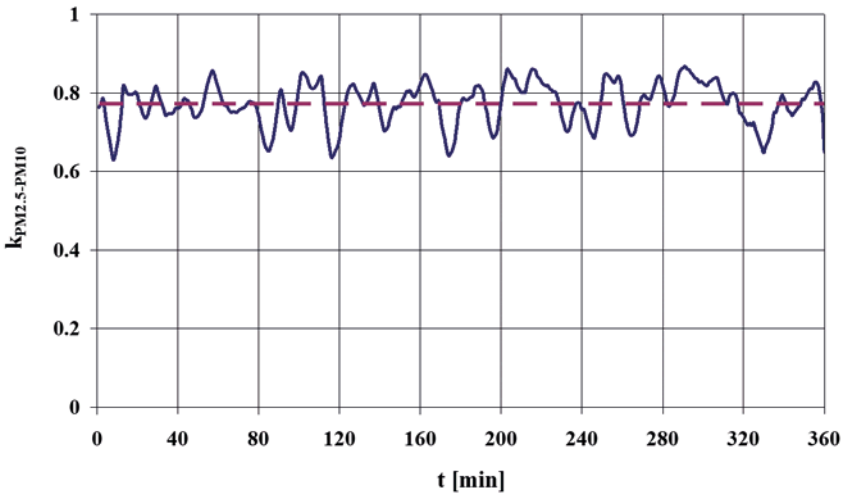

Fig. 14. Coefficient $k_{PM2.5-PM10}$ (data obtained from the Dust Trak DRX Aerosol Monitor) [14]

An analysis of the curves in figures 13 and 14 indicated that the mean value of the coefficient for the model of immission of particulate matter PM1 was high, exceeding 0.95 (data obtained from the Dust Trak DRX Aerosol Monitor). For the model of immission of particulate matter PM2.5, the mean value of the coefficient exceeded 0.75 (data obtained from the Dust Trak DRX Aerosol Monitor) [14].

6. Recapitulation

The research was undertaken to assess the impact of automotive sources of pollutant emission on the values of immission of individual particulate matter size fractions in the atmospheric air in the street canyon in the Warsaw urban agglomeration [14].

The time of carrying out the measurements, i.e. summer season, was chosen on purpose because the air pollution by heating sources is then lower, thanks to which the impact of automotive sources on atmospheric pollution could be presented in a more selective way.

An analysis of the research results has made it possible to ascertain that the immission of particulate matter increases with growing intensity of motor vehicle traffic. It can be seen from the measurement results obtained from the Dust Trak DRX Aerosol Monitor how significant impact is exerted by automotive sources on the values of immission of such pollutants in the atmosphere. Particularly conspicuous were both the cyclic growths and drops in the particulate matter immission resulting from changes in traffic lights' signals and the temporary immission peaks caused by the passage of motor vehicles that emitted a considerable amount of exhaust gases, which could be observed during the measurements [14].

Regrettably, the impact of automotive sources on the values of immission of individual particulate matter size fractions in the atmospheric air could only be roughly estimated on the grounds of the measurements carried out, chiefly because of too short a time of the measurements, but also due to the fact that the measurements were carried out in summer season, when the traffic intensity is reduced [14].

To sum up: the intensity and type of motor vehicle traffic close to air quality monitoring stations should be examined systematically; moreover, the impact of weather conditions on the pollutant immission measurement results should be analysed as well.

In spite of a limited scope of the research carried out, a statement may be made on these grounds that the automotive sources have a significant impact on the air quality in the surroundings and, in consequence, on the health of inhabitants of urban agglomerations [14].

The full text of the article is available in Polish online on the website http://archiwummotoryzacji.pl.

Tekst artykułu w polskiej wersji językowej dostępny jest na stronie http://archiwummotoryzacji.pl.

References

[1] Chłopek Z. Testing of hazards to the environment caused by particulate matter during use of vehicles. Eksploatacja i Niezawodnosc – Maintenance and Reliability. 2012; 2: 160–170.

[2] Chłopek Z. Ocena stanu zagrożenia środowiska przez cząstki stałe PM2,5 ze źródeł transportu drogowego (Evaluation of the state of threat to the environment by the PM2,5 particulates from the road transport sources). Proceedings of the Institute of Vehicles / Warsaw University of Technology. 2011; 82 (1): 101–110.

[3] Chłopek Z. Modelowanie emisji cząstek stałych PM10 ze źródeł motoryzacyjnych do celów oceny oddziaływania transportu drogowego na środowisko (Modelling of the emission of particulate matter PM10 from automotive sources for the purposes of environmental impact assessment of road transport). Report of research project No. N N509 083637 sponsored by the Ministry of Science and Higher Education, Warszawa 2012.

[4] Chłopek Z, Jakubowski A. A study of the particulate matter emission from the braking systems of motor vehicles. Eksploatacja i Niezawodnosc – Maintenance and Reliability. 2009; 4: 45–52.

[5] Chłopek Z, Skibiński F. Wprowadzenie w tematykę emisji cząstek stałych PM2,5 powodowanych transportem samochodowym (Introduction to the subject of the particulate matter emission PM2,5, from the road transport). Transport Samochodowy – Motor Transport. 2010; 3: 73–87.

[6] Chłopek Z, Suchocka K. Analiza przepisów ochrony środowiska przed emisją cząstek stałych w aspekcie ruchu samochodowego (The analysis of environmental protection regulations against particulate matter emission in terms of traffic). Proceedings of the Institute of Vehicles / Warsaw University of Technology. 2014; 97 (1): 21–32.

[7] Chłopek Z, Suchocka K. Modelowanie emisji i imisji frakcji wymiarowych cząstek stałych związanych z ruchem samochodowym (The modeling of emission and immission of particulate matter size fraction related to vehicle traffic). Proceedings of the Institute of Vehicles / Warsaw University of Technology. 2014; 97 (1): 5–20.

[8] Chłopek Z, Suchocka K. Risks posed by particulate matter to the human health and environment near transport routes. The Archives of Automotive Engineering – Archiwum Motoryzacji. 2014; 63 (1): 3–24 and 109–129.

[9] Chłopek Z, Suchocka K, Dudek M, Jakubowski A. Hazards posed by polycyclic aromatic hydrocarbons contained in the dusts emitted from motor vehicle braking systems. Archives of Environmental Protection. 2016; 42 (3): 3–10.

[10] Chłopek Z, Szczepański T. Ocena zagrożenia środowiska cząstkami stałymi ze źródeł cywilizacyjnych (Environmental risk assessment of particulate matter from civilization sources). Inżynieria Ekologiczna. 2012; 30.

[11] Juda-Rezler K. Oddziaływanie zanieczyszczeń powietrza na środowisko (Environmental impact of air pollutants). Oficyna Wydawnicza Politechniki Warszawskiej (Publishing House of the Warsaw University of Technology). Warszawa 2000.

[12] Siemiński M. Środowiskowe zagrożenia zdrowia (Environmental health risk). Wydawnictwo Naukowe PWN. Warszawa 2001.

[13] Sroczyński J. Wpływ zanieczyszczeń powietrza atmosferycznego na zdrowie ludzi (The impact of atmospheric air pollution on human health). Ossolineum Publishing House at the Polish Academy of Sciences. Wrocław 1989.

[14] Strzałkowska K. Sprawozdanie z zadania nr DDS-117-BLM Badania wpływu źródeł motoryzacyjnych na wartość imisji frakcji wymiarowych cząstek stałych w aglomeracji warszawskiej (Report of Project No DDS-117-BLM "Research on the impact of automotive sources on the values of immission of specific particulate matter size fractions in the Warsaw urban agglomeration"). Warszawa 2016.

[15] Suchocka K. Modelowanie imisji cząstek stałych PM2.5 ze źródeł motoryzacyjnych (Modelling of the immission of particulate matter PM2.5 from automotive sources). Engineer's (Bachelor's) graduation work. Warszawa 2012.

[16] Suchocka K. Modelowanie imisji frakcji wymiarowych cząstek stałych ze względu na oddziaływanie motoryzacji na środowisko (Modelling of the immission of specific particulate matter size fractions in respect of the environmental impact of motorization). Master's graduation work. Warszawa 2013.

[17] Żegota M. Modelowanie emisji cząstek stałych PM10 z pojazdów samochodowych (Modelling of the emission of particulate matter PM10 from motor vehicles). Doctoral dissertation. Warsaw University of Technology 2006.